

**Supporting Information for**

**Sodiation vs. Lithiation Phase Transformations in a High  
Rate - High Stability SnO<sub>2</sub> in Carbon Nanocomposite**

*Jia Ding<sup>a\*</sup>, Zhi Li<sup>a</sup>, Huanlei Wang<sup>a</sup>, Kai Cui<sup>b</sup>, Alireza Kohandehghan<sup>a</sup>, Xuehai Tan<sup>a</sup>,*

*Dimitre Karpuzov<sup>c</sup>, David Mitlin<sup>d, a \*</sup>*

<sup>a</sup>Chemical and Materials Engineering, University of Alberta, Edmonton, Alberta T6G  
2V4, Canada

<sup>b</sup>National Institute for Nanotechnology (NINT), National Research Council of Canada,  
Edmonton, Alberta T6G 2M9, Canada

<sup>c</sup> Alberta Center for Surface Engineering and Science (ACSES), University of Alberta,  
Edmonton, AB, Canada T6G 2G6

<sup>d</sup>Chemical & Biomolecular Engineering and Mechanical Engineering, Clarkson  
University, Potsdam, NY, USA 13699

\*Address correspondence to dingjiasi@outlook.com (J. Ding); dmitlin@clarkson.edu (D. Mitlin).

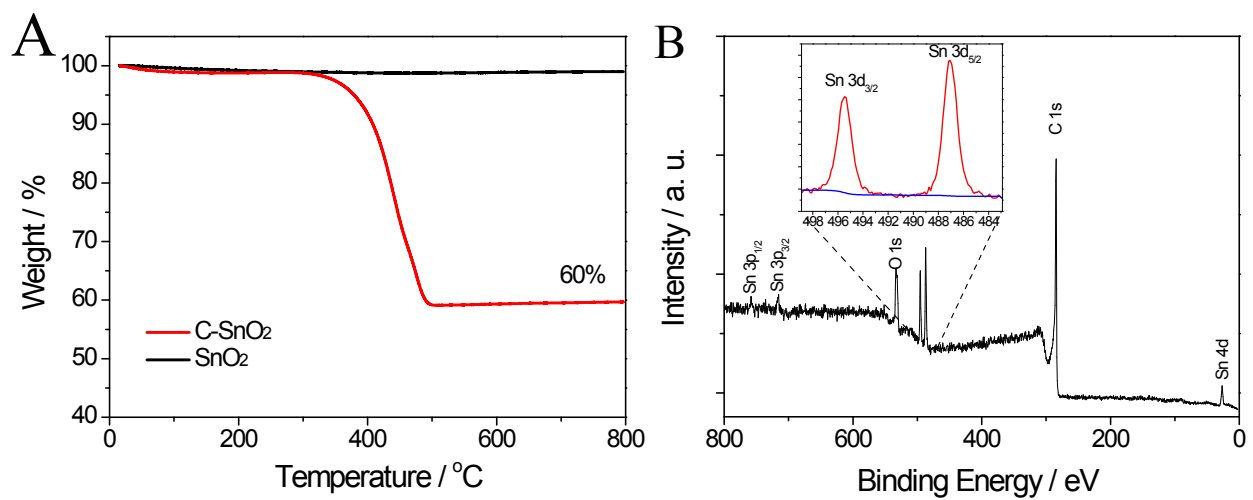


**Figure S1:** (A) Thermogravimetric curves of C-SnO<sub>2</sub> and SnO<sub>2</sub> specimens. (B) XPS survey spectrum of C-SnO<sub>2</sub> and high resolution spectrum of Sn 3d level (insert).

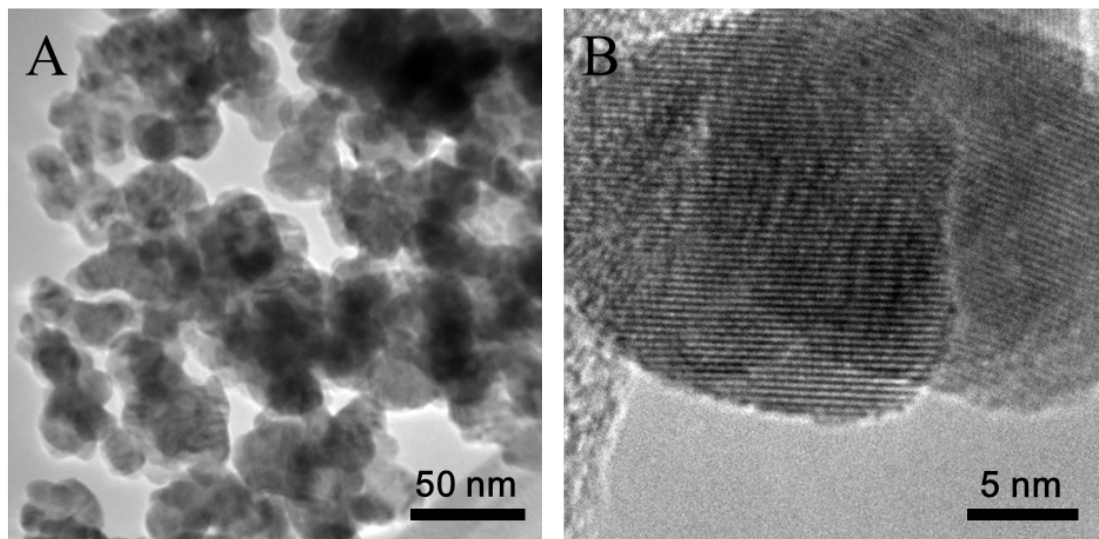


**Figure S2:** (A) Conventional TEM micrograph of the baseline  $\text{SnO}_2$  specimen. (B) HRTEM micrograph of two overlapping  $\text{SnO}_2$  particles.

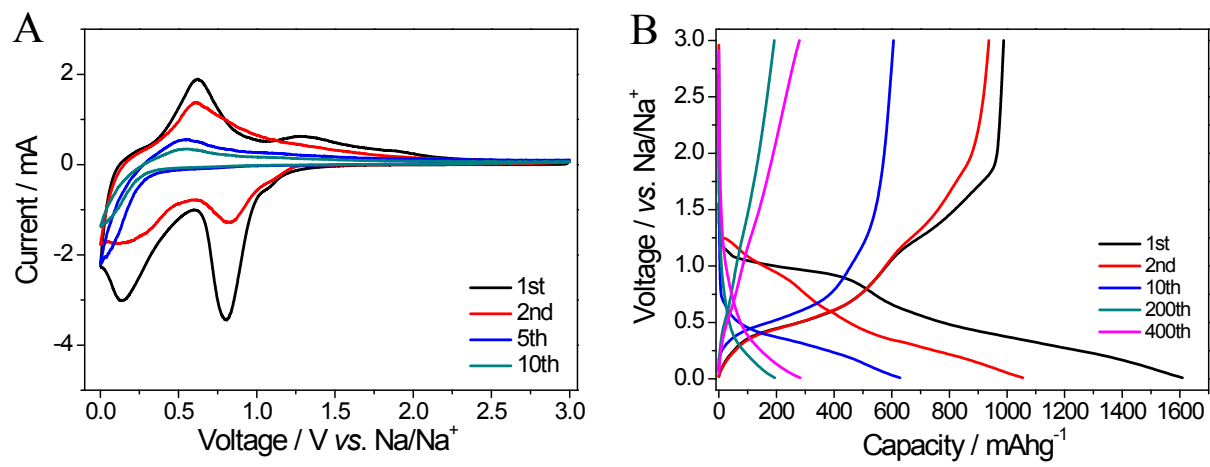


**Figure S3:** Electrochemical performance of  $\text{SnO}_2$  vs. Li. (A) CVs of  $\text{SnO}_2$ , tested at  $0.1 \text{ mVs}^{-1}$ . (B) Galvanostatic discharge/charge profiles of  $\text{SnO}_2$ , tested at  $0.5 \text{ Ag}^{-1}$ .

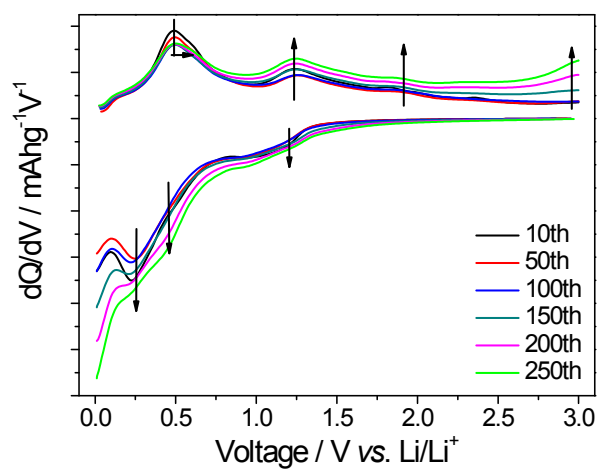


**Figure S4:** Derivate curves  $dQ/dV$  vs.  $V$  for C-SnO<sub>2</sub> electrode against Li.

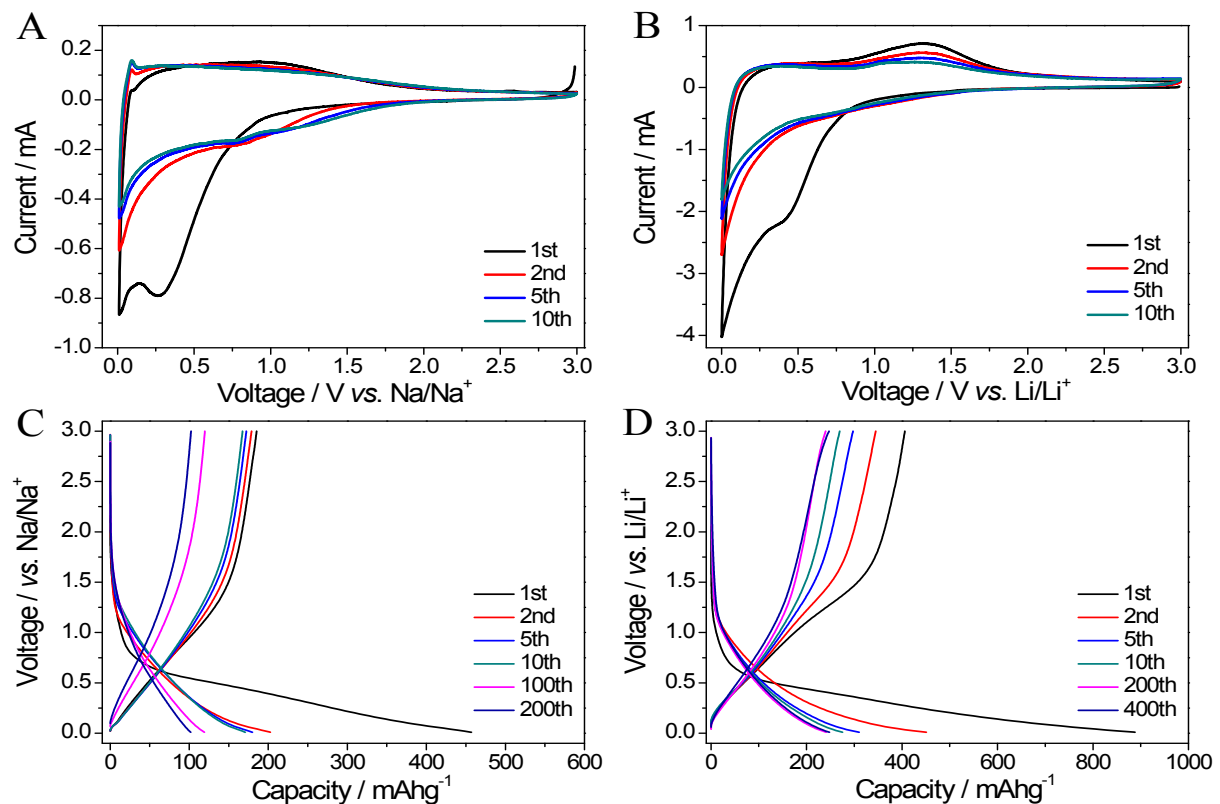


**Figure S5:** Electrochemical performance of pure carbon in a half-cell vs. Na, Li. (A) CVs of pure carbon electrode for the cycle 1 – 10 vs. Na, tested at  $0.1 \text{ mVs}^{-1}$ . (C) Galvanostatic discharge/charge profiles of pure carbon electrode, tested at  $0.08 \text{ Ag}^{-1}$ . (B) CVs of pure carbon electrode for the cycle 1 – 10 vs. Li, tested at  $0.1 \text{ mVs}^{-1}$ . (D) Galvanostatic discharge/charge profiles of pure carbon electrode, tested at  $0.5 \text{ Ag}^{-1}$  vs. Li.

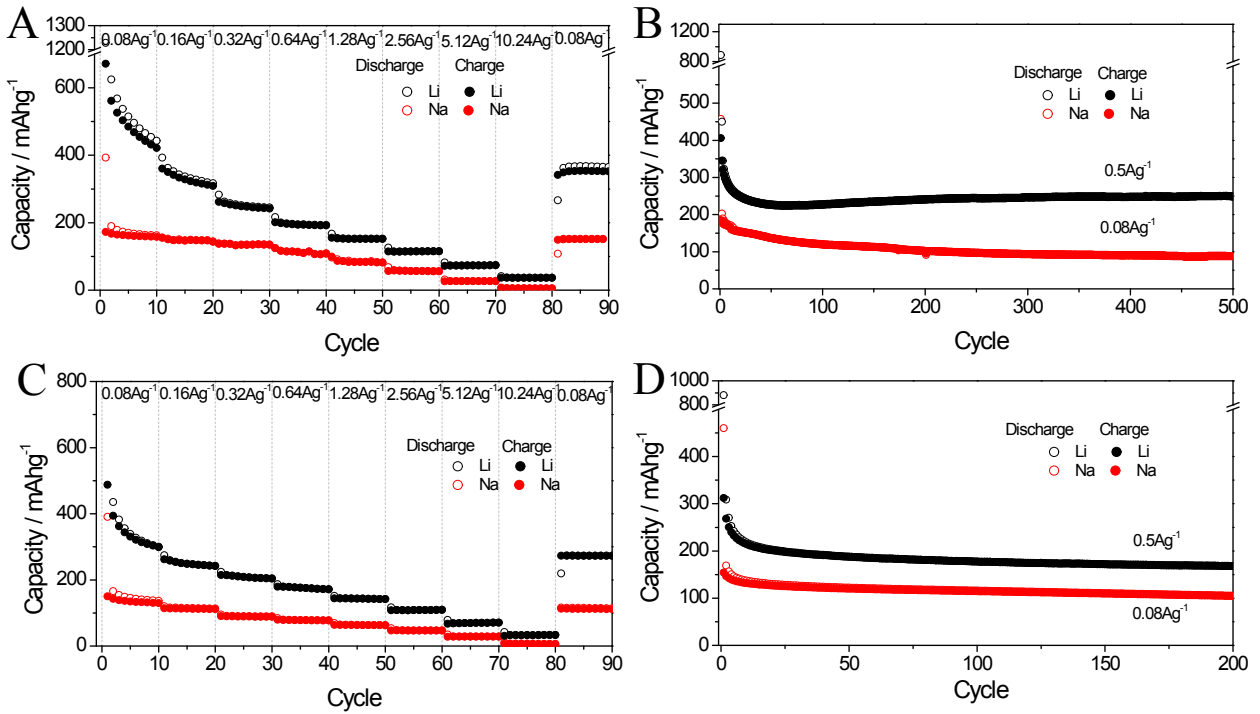


**Figure S6:** (A) Rate performance of the baseline pure amorphous carbon electrodes vs. Na and vs. Li, tested 0.01-3V. (B) Cycling performance of pure carbon electrodes, tested 0.01-3V. (C) Rate performance of the baseline pure amorphous carbon electrodes vs. Na and vs. Li, tested 0.01-1.5V. (D) Cycling performance of pure carbon electrodes, tested 0.01-1.5V.

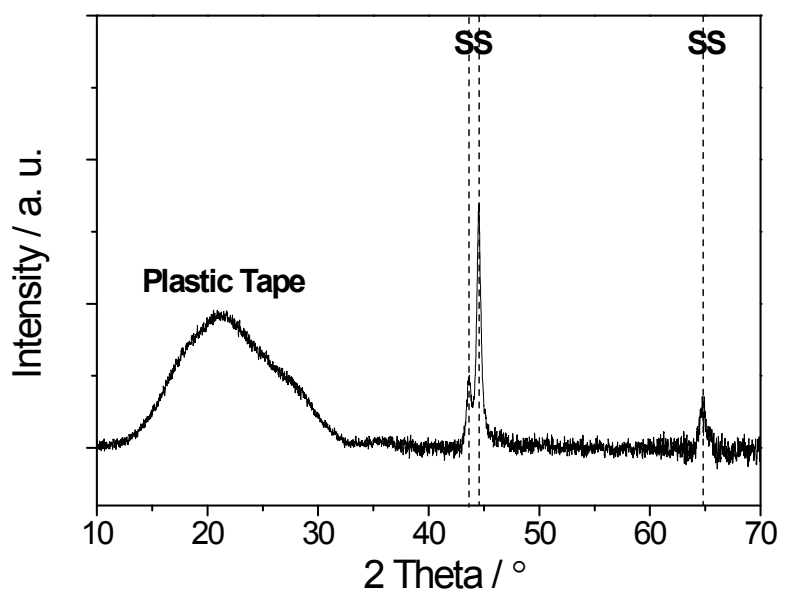


**Figure S7:** XRD pattern for the plastic tape on the stainless steel current collector.

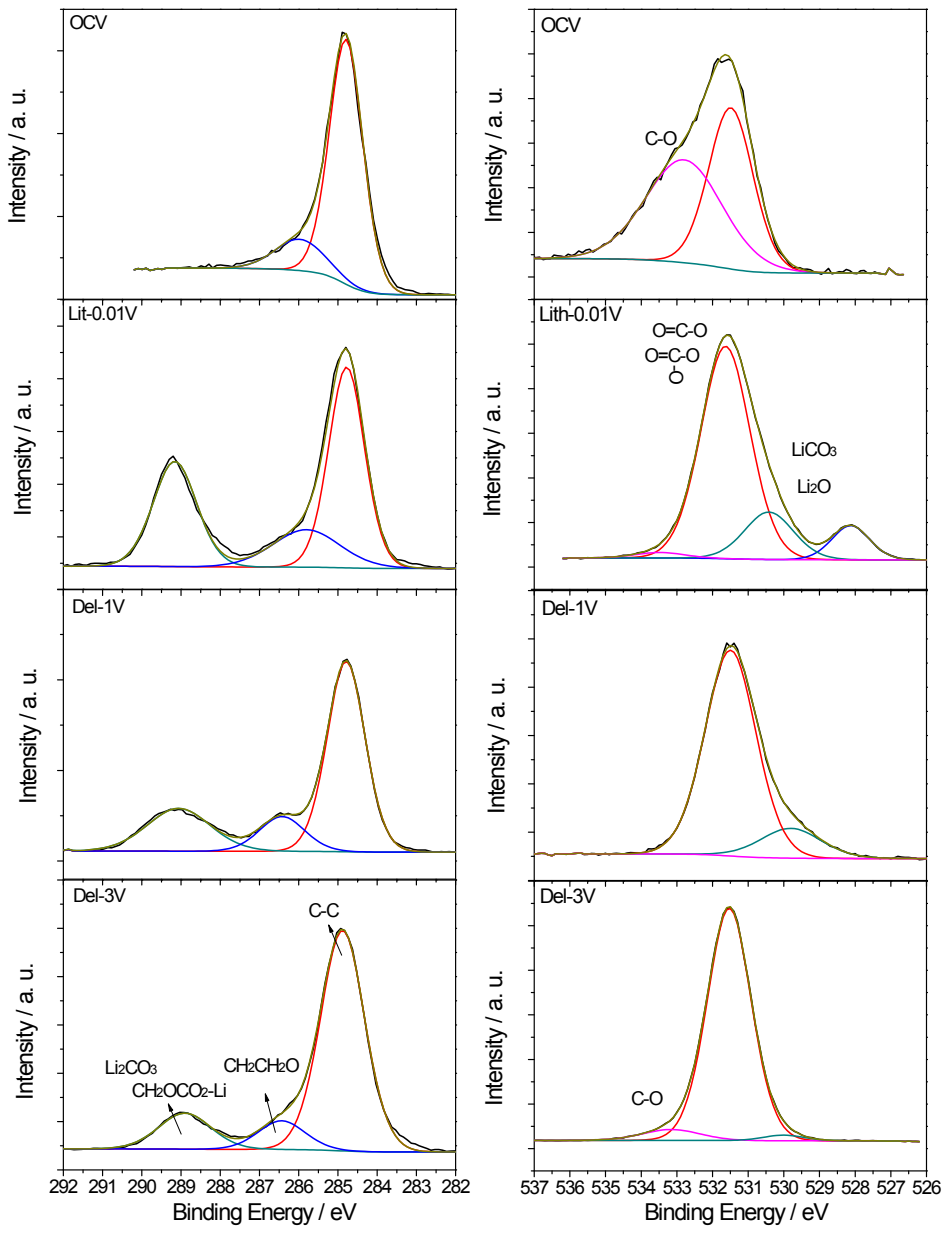
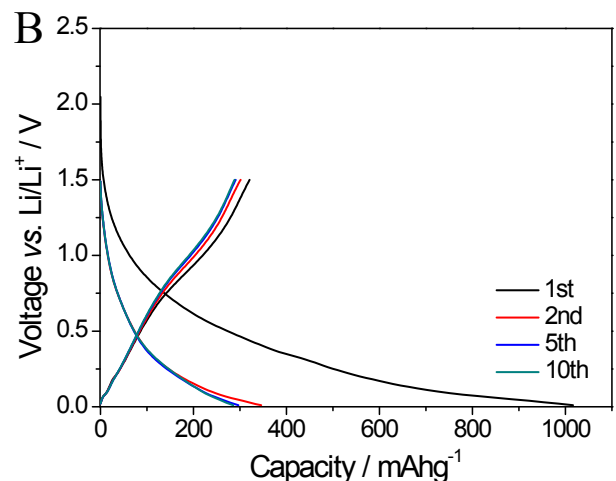
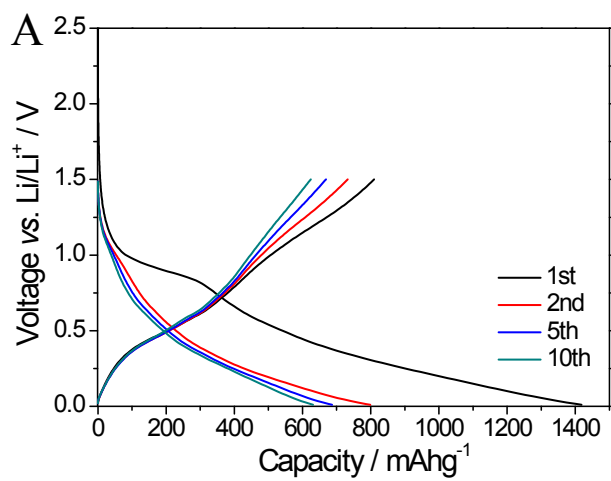


**Figure S8:** XPS spectra for C 1s (left) and O 1s (right) of C-SnO<sub>2</sub> electrodes at the same cut-off voltages.



(A) and Na (B) between 0.01 and 1.5V tested at current density of  $80\text{mA g}^{-1}$ .

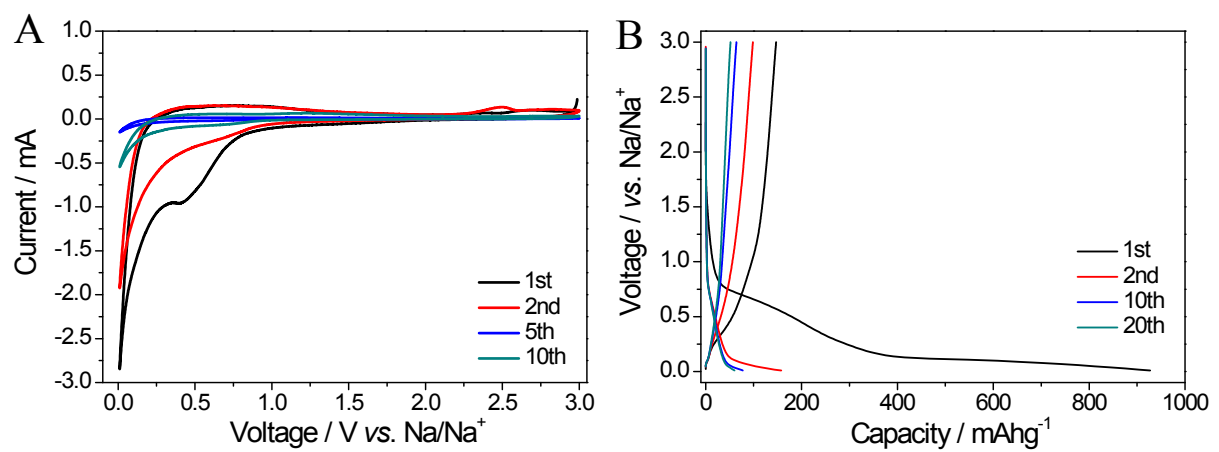


**Figure S10:** Electrochemical performance of  $\text{SnO}_2$  versus Na. (A) Cyclic voltammograms (CVs) of  $\text{SnO}_2$  electrode. (B) Galvanostatic discharge/charge profiles of  $\text{SnO}_2$  electrode at current density of  $0.08 \text{ Ag}^{-1}$ .

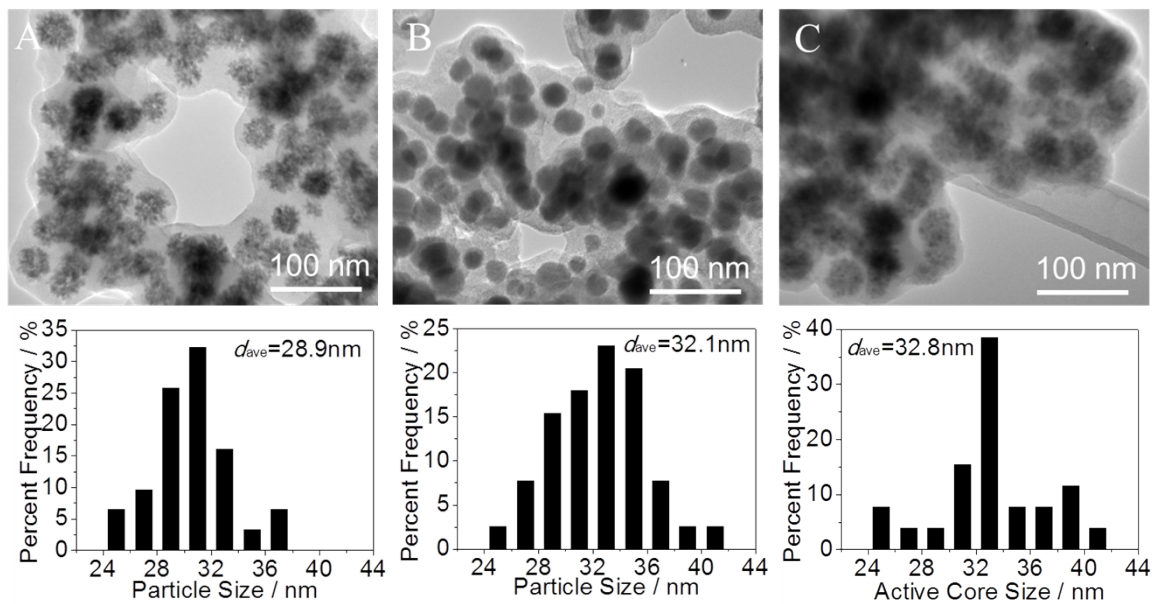


**Figure S11:** (A-C) TEM micrographs of C-SnO<sub>2</sub> with corresponding histograms for the size of the active SnO<sub>2</sub> nanocrystal assemblies (not individual crystallites). (A) Open circuit potential. (B) Sodiated to 0.01V. (C) Desodiated to 3V.

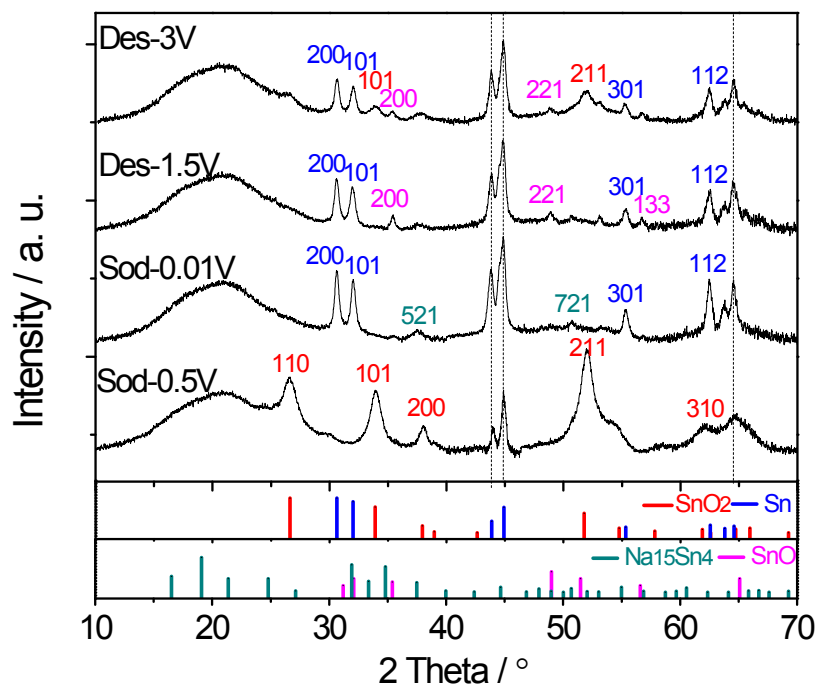


**Figure S12:** (A) XRD patterns of SnO<sub>2</sub> electrodes at various cut-off voltages: first sodiation to 0.5V, first sodiation to 0.01 V, first desodiation to 1.5V, first desodiation to 3V.

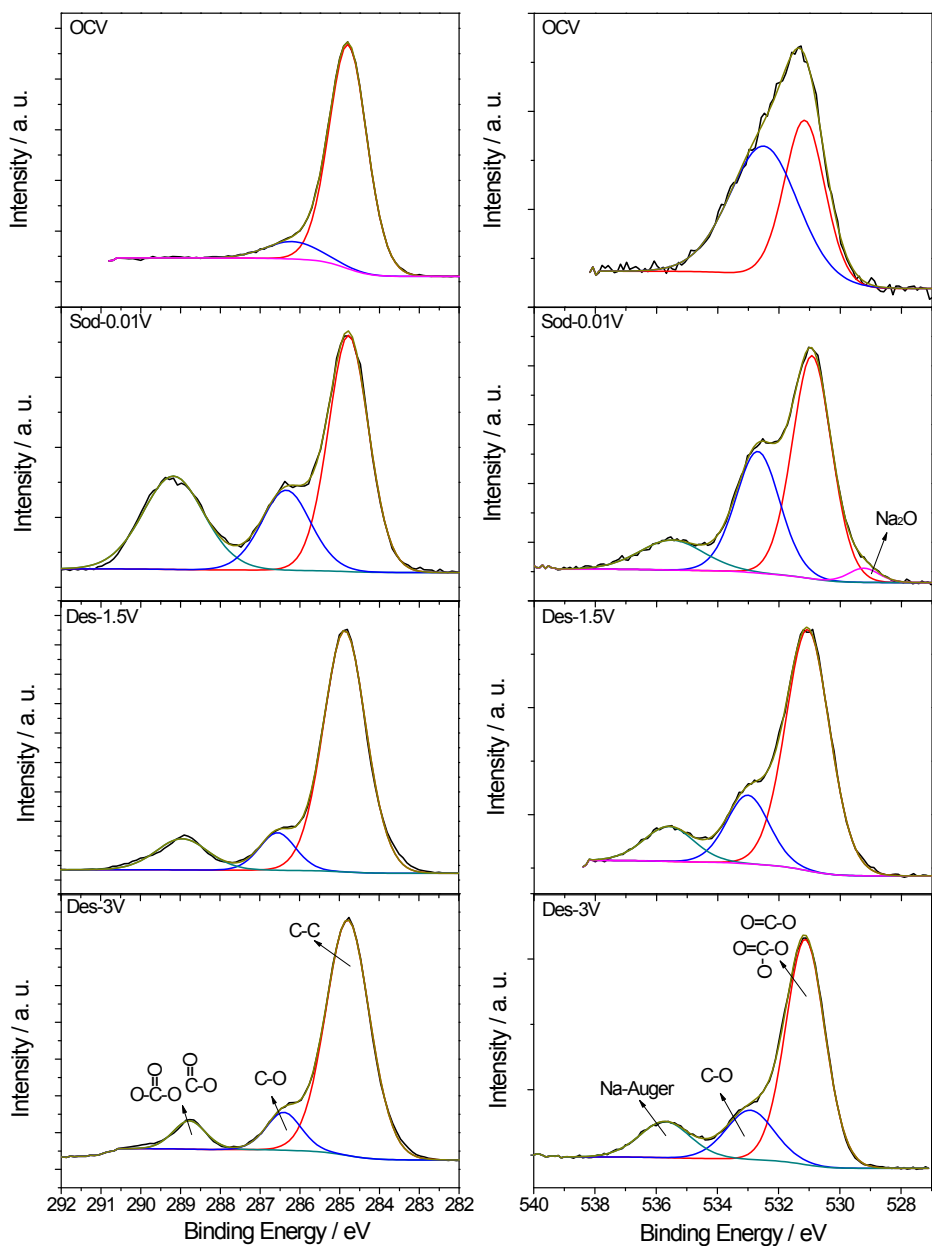


**Figure S13:** XPS spectra for C 1s (left panel) and O 1s (right panel) levels of C-SnO<sub>2</sub> electrodes at various cut-off voltages (open circuit voltage, first sodiated to 0.01 V, first desodiated to 1.5V, first desodiated to 3V vs. Na/Na<sup>+</sup>).